

# Numerical Analysis of Two Models of Air Deflectors to Improve the Aerodynamics of a Heavy Truck

Moussa Amadji<sup>(1\*)</sup>, Djamel Haddad<sup>(1)</sup>, Hamza Benyahia<sup>(2,3)</sup>

<sup>(1)</sup> Institute of Industrial Hygiene and Safety, University of Chahid Mostapha Ben Boulaid Batna 2, Batna 05000, ALGERIA

e-mail: [m.amadji@univ-batna2.dz](mailto:m.amadji@univ-batna2.dz)\*

e-mail: [d.haddad@univ-batna2.dz](mailto:d.haddad@univ-batna2.dz)

<sup>(2)</sup> ENSTA Bretagne, IRDL - UMR CNRS 6027, F-29200 Brest, FRANCE

<sup>(3)</sup> Clément Institute (ICA), University of Toulouse, CNRS UMR 5312, INSA, ISAE-Supaéro, INSA, IMT Mines Albi, UPS, FRANCE

e-mail: [hamza.ben\\_yahia@ensta-bretagne.org](mailto:hamza.ben_yahia@ensta-bretagne.org)

## SUMMARY

Fuel consumption and pollutant gas emissions are major issues that affect the heavy-duty truck industry. The installation of air deflectors on the roof of truck cabins is a widely adopted strategy to reduce drag and improve aerodynamics. The latter is directly related to fuel consumption and pollutant gas emissions. This study aims to identify the optimal air deflector design to improve aerodynamic performance. Seven vehicle body configurations were modelled using SolidWorks 3D design software: a basic model (truck without a deflector) and six models equipped with deflectors. Computational fluid dynamics (CFD) analyses were conducted for each configuration to determine the most aerodynamically efficient structure. The results reveal that models with air deflectors achieved reductions in static pressure (ranging from 0.17% to 1.73%) and velocity (ranging from 1.2% to 5%) compared to the basic model. These findings confirm the critical role of air deflectors in enhancing aerodynamic performance and reducing drag force. Among the different models, the first deflector (case 1) stands out for its best performance, with an estimated drag coefficient reduction of 19.80% and a corresponding decrease in fuel consumption of 19.79%. In conclusion, these results show that drag reduction directly impacts fuel economy.

**KEYWORDS:** air deflector; drag coefficient; fuel saving; velocity; truck.

## 1. INTRODUCTION

Heavy-duty articulated vehicles and heavy-duty trucks are commonly used to transport goods between major cities via highways. The popularity of these large commercial vehicles is mainly due to their flexibility and transport efficiency [1]. Typical diesel engines used in these trucks have an average thermal efficiency of about 33%, which means that about 33% of the fuel is converted into useful energy, measured at the engine output shaft [2, 3]. The remaining 67% is

lost as heat, either through the exhaust and cooling system or due to engine friction. A small portion of the engine's useful energy is used by the powertrain and transmission, and the remaining portion is used to propel the vehicle and operate auxiliary loads such as the alternator, air compressor, and hydraulic fans. To propel the vehicle forward, the engine must provide enough power after compensating for these losses to overcome inertia, gravity, drag, and rolling resistance [4].

With the reduction of crude oil inventories and the improvement of environmental standards, it has become crucial to optimize efficiency and reduce fuel consumption in vehicle design [5]. Reducing the drag coefficient has proven to be a key strategy to reduce the fuel consumption of heavy-duty trucks. When a heavy-duty truck travels on the highway at  $100\text{ km/h}$ , aerodynamic drag accounts for at least 52% of the total fuel consumption [6].

Reducing the drag of heavy-duty vehicles can significantly improve fuel efficiency and, therefore, contribute to the reduction of air pollution caused by exhaust gases. Several aerodynamic solutions have been proposed to effectively reduce drag, including the cab roof fairing (or wind deflector) [7]. The roof wind deflector is an aerodynamic component mounted on the roof of the truck cab to reduce the total air resistance of the truck. The deflector, by definition, is a device designed to change the direction of a flow [8]. The deflector not only improves the aerodynamic characteristics but also enhances the driving stability of the vehicle, which provides guidance for practical technical applications [9]. In addition, wind deflectors also contribute to road safety. By improving the stability of trucks against crosswinds, they reduce the risk of serious accidents, such as rollovers, which can occur when these massive vehicles are exposed to adverse wind conditions. Thus, wind deflectors are not only essential for fuel efficiency but also for environmental protection and road transport safety [9].

Manufactured roof deflectors are designed, engineered, and manufactured to improve the aerodynamics of all light and heavy industrial vehicles. Combining technology and design, they give the truck a performance profile that offers minimal air resistance. The benefits of an air deflector can be outlined in the following points.

- Reduced fuel consumption
- Increased engine life
- Improved fuel efficiency
- Reduced engine and transmission wear
- Reduced truck maintenance
- Improved stability
- Reduced projections
- Ideal for sign writing and advertising space
- Individual style to suit each truck model

The presence of the deflector allows a much cleaner air flow at the junction between the cab and the trailer. Its presence results in a 19% reduction in drag, which directly reduces fuel consumption [10, 11].

## 1.1. RELATED WORK

Reducing aerodynamic drag is closely linked to fuel consumption and CO<sub>2</sub> emissions, making it a critical area of research for various vehicle types, including light vehicles, heavy-duty trucks, and trains [9]. Among the primary factors affecting aerodynamic drag, vehicle shape plays a pivotal role [12]. The flow of air around a vehicle is significantly influenced by its geometry, with contours, angles, and sharp edges impacting both drag and lift.

Approximately half of a vehicle's total aerodynamic drag originates from airflow around the front of the vehicle and the gap between the tractor and trailer in articulated trucks. Consequently, airflow control devices designed to mitigate drag at the front of heavy vehicles are of substantial practical significance. The cab roof fairing (CRF) is one of the most widely adopted drag reduction devices, typically installed on the roof of trucks or semi-trailers [11].

Jeong Jae Kim et al. [11] compared three deflector models (Cab roof fairing, CRF) using numerical calculations (coarse large eddy simulation, LES) and wind tunnel studies. According to their research, altering the deflector (third model) resulted in notable modifications to the flow structure and a roughly 19% decrease in drag. They compared the flow characteristics around the front of the vehicle with and without a deflector using the PIV (particle image velocimetry) flow field measurement.

P. Nishanth et al [13] studied the effects of a passive flow control device and a rear extension on overall drag reduction. They designed a full-scale bus model and performed a CFD analysis on ANSYS Fluent using the k- $\omega$  model to determine the drag generated by the bus. They observed that the drag decreased with increasing angle until it reached a minimum value, after which it began to increase. This variation was attributable to airflow separation that occurred at higher angles of rear extension inclination. They also manufactured reduced models (at a scale of 1:20) by 3D printing for experimental validation. Flow separation occurred between 15° and 18°. They found that the tail of the bus, 500 mm long and tilted at an angle of 12°, presented an optimal balance between drag reduction and practicality.

By altering three frontal nose models of the train known as the Mask of Car (MoC), B. Halfina et al. [14] created a model of a high-speed train (HST). To determine the ideal shape, they employed the intricate 3D model's curvature properties, including side surface curvature, top surface curvature, and nose length. Using Ansys Fluent software, the models were constructed at full scale and then simulated using computational fluid dynamics (CFD). The goal of this research is to provide an ideal design approach by using a numerical method to examine the drag coefficient of various HST mask forms for automotive design. They discovered that the longer, sharper snout of the MoC lowers drag from the air. In conclusion, the aerodynamic design of high-speed train cars should give particular consideration to nose length and slenderness, since these parameters significantly influence drag reduction. Mohamed B. Farghaly et al. [15] used experimental and digital methods to examine the effects of various drag reduction devices geometric parameter changes on the aerodynamics of a truck at an airflow speed of around 20 m/s. To determine the percentage of improving drag reduction, the standard truck profiles were evaluated both with and without the drag reduction devices. The results show that installing all additional devices simultaneously reduces the drag coefficient by approximately 59 % compared to the baseline truck.

Given the existence of several types of air deflectors, we selected two models and installed them in three different positions, resulting in six configurations. The aim of this study is to identify the

optimal configuration among these six to achieve drag coefficient reduction using computational fluid dynamics (CFD).

The paper is organized into four sections. The first section emphasizes the importance of heavy-duty trucks in transportation and outlines key properties of typical diesel engines used in these trucks. It also discusses the direct relationship between drag coefficient and fuel consumption, highlighting the role of air deflectors in reducing the drag coefficient, improving truck aerodynamics, achieving fuel savings, and mitigating air pollution from exhaust gases. Finally, this section presents a review of related works.

The second section describes the base model, the six variants of models equipped with air deflectors, the dimensions of the virtual wind tunnel, mesh convergence, boundary conditions, and the theoretical background to fuel consumption.

The third section presents the simulation results with figures of streamlines, turbulent kinetic energy, velocity contours surrounding each model, and pressure concentration zones.

The fourth section summarizes the study's findings and highlights the primary benefits of using air deflectors.

## 2. MATERIALS AND METHODS

### 2.1. GEOMETRIC MODEL

To model the trucks as realistically as possible, we used the dimensions of a model available in the online library GrabCAD [16], shown in Figure 1-a. The model measures  $9100\text{ mm}$  in length,  $2400\text{ mm}$  in width and  $3616\text{ mm}$  in height. The heavy truck model was designed using the 3D modelling software SolidWorks 2019. Figure 1-b illustrates the transformation of the complex shape into a simplified solid model suitable for simulation.

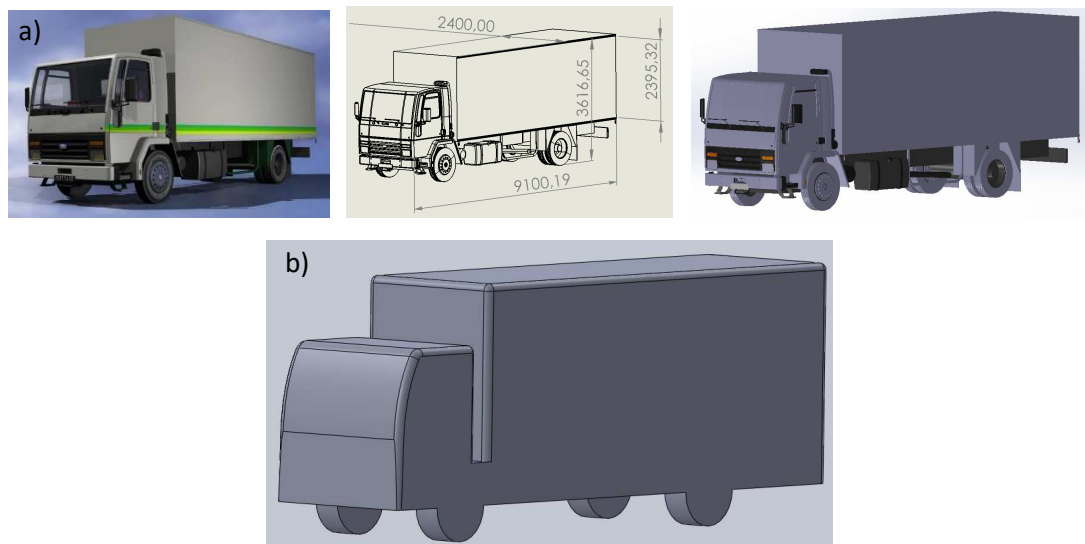


**Fig. 1** Actual truck dimensions, a) the existing model [16], b) the simplified heavy truck model

Due to constraints related to model dimensions and computational accuracy, many details of the vehicle body, such as front headlights, windshield wipers, mirrors, and door handles, were

simplified. An overly realistic modelling of those models would have required an excessively fine mesh in regions not relevant to this study, thus greatly increasing the computational time. For example, the wheels were modelled as simple cylinders, since accurately capturing the complex flow behind each hub cap would have required a very fine mesh in this area.

Furthermore, the aim of this paper was to study the flow of the truck in a manner consistent with previous studies [11, 13, 14, 17], and to compare two deflector models in three different positions in order to find the optimal shape.

Figure 2 illustrates the two air deflector models in three different positions. In the first configurations, the height of the deflector is lower than that of the container. In the second, the height of the deflector is at the same height as that of the container. Finally, in the third, the height of the deflector is higher than that of the container.

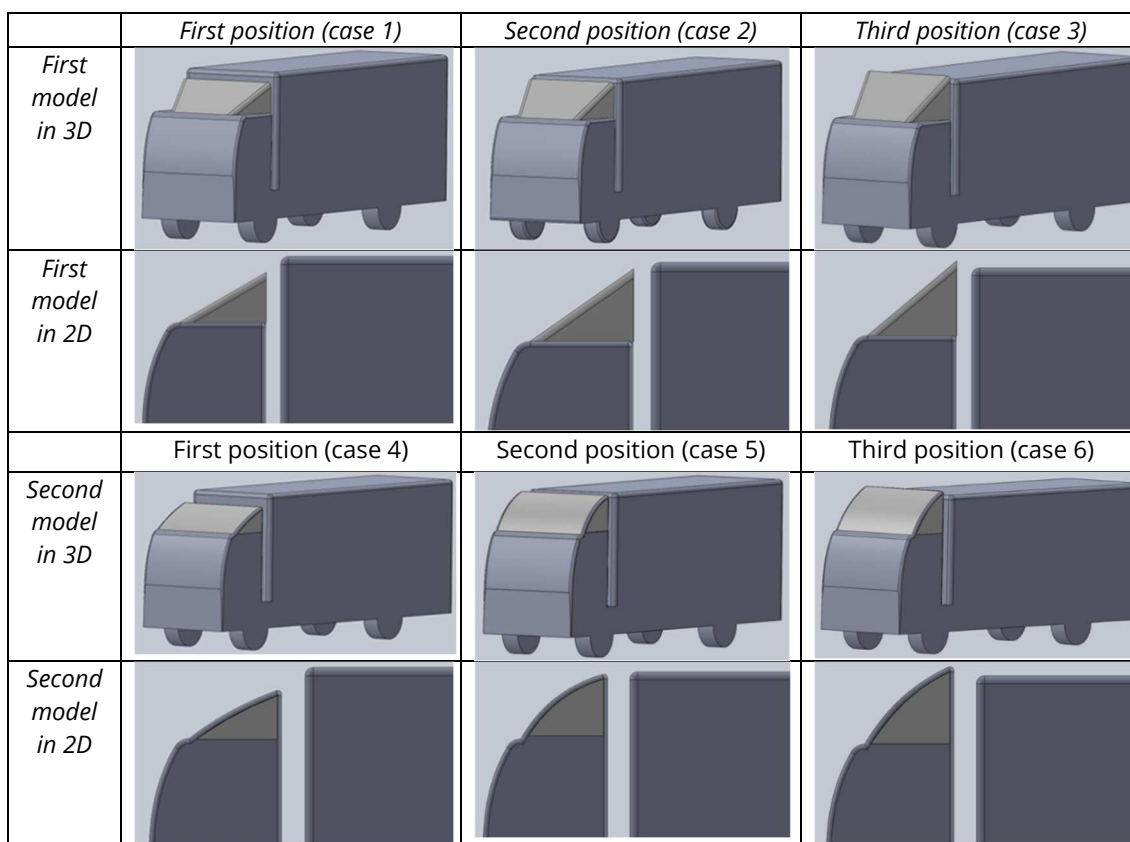


**Fig. 2** Three-dimensional and Two-dimensional representations of both Models in three configurations

## 2.2. NUMERICAL ANALYSIS TECHNIQUES

The CAD models of the truck, both with and without air deflectors, were imported into ANSYS Workbench® simulation software (ANSYS Inc, 2023) to create a virtual wind tunnel. This virtual wind tunnel, represented as a cuboid enclosing the truck model (Figure 3) has dimensions of 110 m in length, 20 m in width, and 13 m in height.

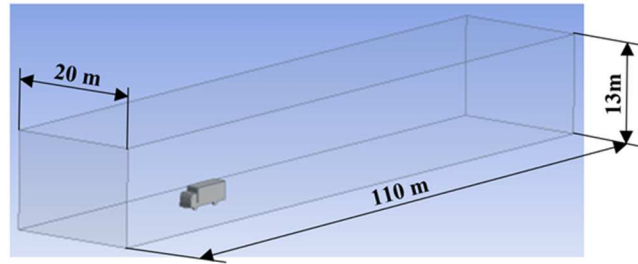


**Fig. 3** Dimension of the computational domain and enclosure

The computational domains of the models are discretized with unstructured hybrid meshes consisting of tetrahedral and prismatic elements. To improve the accuracy of the digital simulation, the meshes around the truck models are refined.

Furthermore, the convergence of the basic model numerical simulation (truck without deflector) is presented in Figure 4.

A convergence study was carried out five differently sized elements (2000, 1500, 1000, 750, 500 mm). It was observed that beyond the element size of 750 mm, the drag coefficient stabilizes at the value of 0.515 (Figure 4).

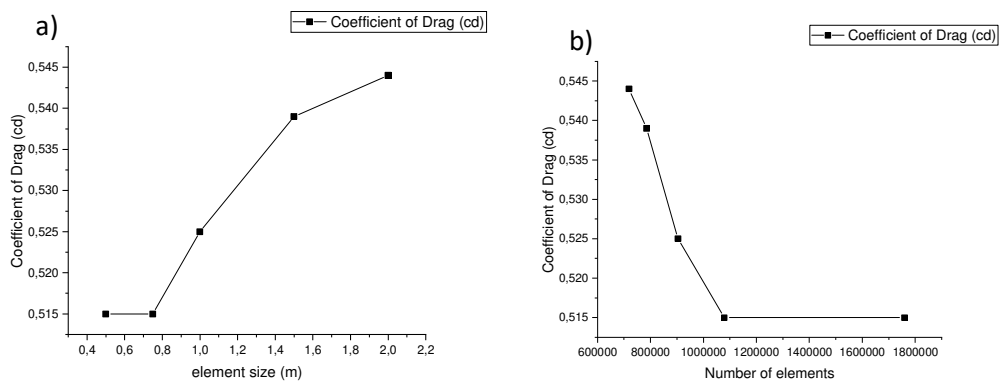


**Fig. 4** Meshes convergence, (a) coefficient of drag as a function of element size, (b) coefficient of drag as a function of number of elements

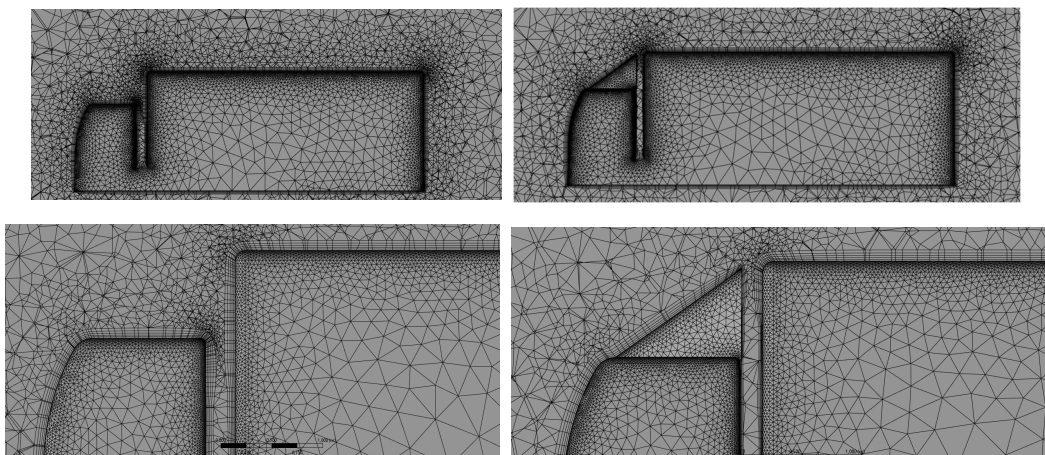


**Fig. 5** Mesh details of two models with inflation layers

The employed mesh has an element size of  $500\text{ mm}$ , with a total of  $1759858$  elements and  $397656$  nodes for the truck model without deflectors. The mesh details are shown in Figure 5. In this simulation, the boundary layers on the truck surface were considered using an inflation meshing strategy. These layers have a total thickness of  $100\text{ mm}$  distributed across five layers. The velocity vectors, the magnitude of the pressure near the surface, and the associated parameters can be observed.

Table 1 presents the number of elements and nodes for each analysis case.

**Table 1** Number of elements and nodes for each analysis case

	Case 1	Case 2	Case 3	Case 4	Case 5	Case 6
Number of elements	1808352	1811798	1816246	1853696	1874666	1877740
Number of nodes	413526	414738	415350	425826	432415	432835

### 2.3. BOUNDARY CONDITIONS AND SOLVER SETTINGS

To investigate the aerodynamic characteristics of the truck with and without an air deflector, CFD simulations of the proposed models were performed in the virtual wind tunnel using Ansys Fluent 2023.

The numerical analysis was carried out at the target operating speed of  $110\text{ km/h}$ , approximately  $30\text{ m/s}$ . The Reynolds number calculated on the truck speed of  $V=30\text{ m/s}$ , air density of  $\rho=1.225\text{ kg/m}^3$ , and kinematic viscosity  $\nu=1.7894\times 10^{-5}\text{ m}^2/\text{s}$  using the following equation:

$$Re = \frac{\rho VL}{\mu} = \frac{VL}{\nu} \tag{1}$$

$V$  - Velocity of the fluid

$L$  - The characteristic length, the chord width on an airfoil

$\rho$  - The density of the fluid

$\mu$  - The dynamic viscosity of the fluid

$\nu$  - The kinematic viscosity of the fluid

$$Re=4.023\times 10^6$$

This indicates the presence of turbulence in the flow. The conventional three-dimensional incompressible  $k-\epsilon$  model, derived from the transport equations for the kinetics of turbulence energy ( $k$ ), was employed as the turbulence model in this study.

#### Fuel Consumption Analysis

Drag is the force acting on a vehicle that opposes its motion through the air. This force is therefore directly related to vehicle’s aerodynamic characteristics. Consequently, it is in the interests of manufacturers to minimize drag, as it increases fuel consumption and reduces line speed. Drag acts in the horizontal, a rearward direction and its point of application is located at the vehicle’s centre of gravity. To assess the effects of air deflector on truck drag reduction, we compare the results of the CFD simulation of the base vehicle (truck without deflector) with those of the vehicle equipped with an air deflector, as shown in Figures (6-13). Aerodynamic drag is generally calculated using the following formulation [18, 19]:

$$F_{drag} = \frac{1}{2} \rho \cdot C_d \cdot A_f \cdot V^2 \tag{2}$$

$\rho$  - Density of air in  $kg/m^3$  (approximately  $1.2 kg/m^3$ , density varies with pressure, temperature and humidity).

$V$  - Vehicle speeds in relation to air in  $m/s$  (if the wind blows from the front, the vehicle speed is added to that of the wind; and if it blows from behind, the wind speed is subtracted from the vehicle speed).

$A_f$  - The maximum frontal area of the vehicle, expressed in  $m^2$ , is approximated using the following formula:  $A_f = 0.9 l h$ , with  $l$ , the width of the vehicle at the front and  $h$ , the total height of the vehicle.

$Cd$  - Drag coefficient ( $Cd$  of vehicles varies between  $0.04$  and  $0.7$ ).

It is stated that the total effect of all the elements causing aerodynamic drag is represented by the drag coefficient, or  $Cd$  [20]. Therefore, the aerodynamic drag performance of the truck with and without an air deflector is assessed using the drag coefficient as an indicator.

A numerical analysis was carried out to compare fuel consumption with the drag force produced by the Ansys Fluent simulation. This comparison examines the amount of fuel required to overcome the vehicle's drag.

According to Ainul Ghurri et al. [21], the following equations can be used to numerically represent the relationships between drag force and fuel consumption:

$$Pw = F_{drag} \cdot V \quad (3)$$

$$E = \frac{P}{V_{truck}} \quad (4)$$

$$F_c = \frac{E}{\Phi d} \quad (5)$$

where  $V_{truck}$  is the truck speed (km/h),  $F_c$  is the fuel consumption (L/km),  $F_{drag}$  is the drag force (N),  $Pw$  is the power required to overcome drag (W),  $E$  is the energy consumption per kilometer-hour (Wh/km),  $\Phi d$  is the specific energy of the fuel (Wh/L). In this investigation, truck fuel is diesel with a specific energy of  $10.6 \times 10^3 Wh/L$  was used [22].

### 3. RESULTS AND DISCUSSION

Numerical simulations were conducted using ANSYS Fluent to investigate the effects of two deflector designs in three distinct positions on the drag coefficient, static pressure, velocity, and other aerodynamic parameters.

Analysis of the baseline truck model revealed that static pressure constituted a significant proportion of the aerodynamic forces compared to models equipped with deflectors. Figure 6 illustrates the pressure distribution contours around the baseline model. The static pressure generated by the baseline model was measured at  $575 Pa$ , primarily concentrated on the windshield and the upper section of the container. Figures 6 and 7 demonstrate that, in the absence of a deflector, the stagnation line impacts the front face of the container, resulting in a pronounced high-pressure region. Conversely, when a deflector is installed, the airflow is effectively redirected, eliminating stagnation on the front face and preventing flow penetration into the container space [23].

Figure 7 shows the pressure distribution contour around the two models in three positions. It was observed that the pressure was mainly concentrated on the windshield in all cases studied. Moreover, it was also evident at the upper part of the container in two models for the first position (Cases 1 and 4). The pressure values in all cases (both models in three positions) were

lower than that of the basic model. After analysing the pressure values, it was found that the following three cases: the second model in the third position (case 6), the second model in the first position (case 4), and the first model in the second position (case 2) produced the lowest pressure values, respectively 565, 566, and 567 Pa. This resulted from differences in the air deflector shape and the installation position.

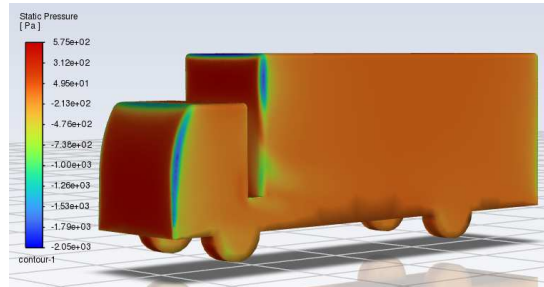


Fig. 6 Pressure contour on the basic model

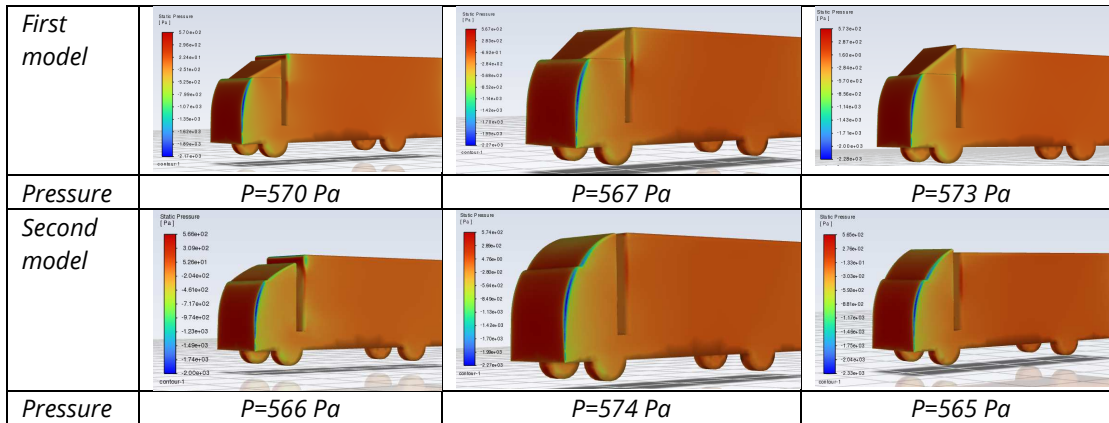


Fig. 7 Comparison of pressure distribution in different cases

The analysis of the velocity contours around the truck revealed that, without a drag reduction device (deflector), the airflow over the vehicle had an unfavourable distribution, characterized by a dominance of low-speed areas, which increased the drag force. Areas of flow recirculation appeared particular at the front of the cabin, above the container and at the rear of the container, as shown in Figure 8. These recirculation zones, caused by sharp edges, contributed to the overall drag increase. In contrast, with the addition of an air deflector, the intensity of flow separation was considerably reduced, leading to improved flow distribution around the truck, as shown in Figure 9, and therefore to a significant decrease in drag [15, 21]. Research conducted by KHOSRAVI Mehrdad et al [24] confirmed that when the truck was not equipped with the drag reduction device, the drag force increased due to the high pressure acting on the vehicle's surface.

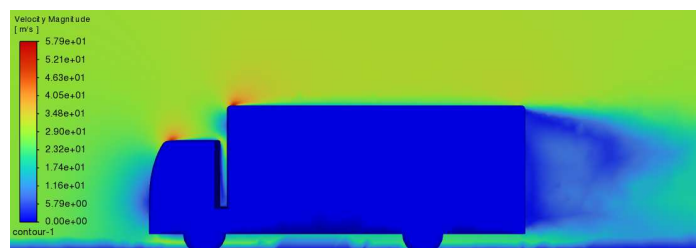
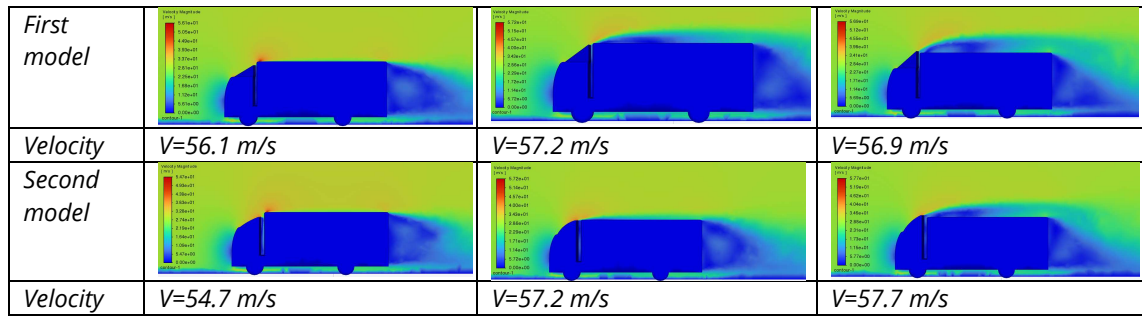
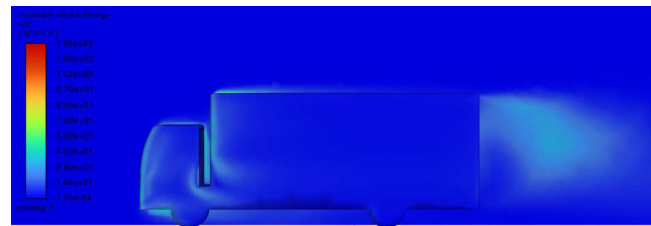


Fig. 8 Velocity contour on the basic model



**Fig. 9** Comparison of velocity contour distribution in different cases

The turbulent kinetic energy was compared to investigate the unsteady flow characteristics over the truck with and without a deflector (Figures 10, 11).



**Fig. 10** Turbulent kinetic energy contour on the basic model

The distribution of turbulence kinetic energy contours around the truck body, both with and without an air deflector, is shown in Figures 10 and 11.

From Figure 10, high turbulence kinetic energy is observed in front of the cabin, above its surface, in the space between the cabin and the container, above and behind the container. This high turbulence causes the formation of vortices due to a strong adverse pressure gradient and flow separation occurring near the edges.

Figure 11 shows the variation of turbulence kinetic energy contours around the truck body equipped with an air deflector (in six studied cases).

In Case 1, the flow around the body is smoothed due to the favourable shape and position of the deflector. In cases 2 and 3, the contours of the turbulence kinetic energy are mainly located above the container, with acceptable values. On the other hand, in cases 5 and 6, these contours appear almost all around the truck body. Finally, in case 4, a high turbulence kinetic energy is observed between the cabin and the container.

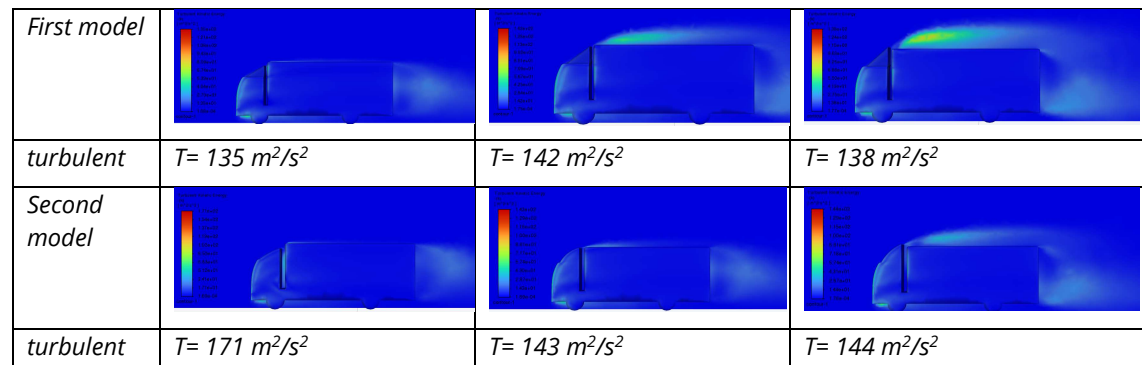
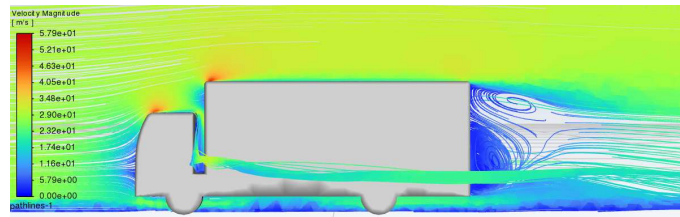


**Fig. 11** Comparison of turbulent kinetic energy contour distribution in different cases

Streamlines are defined by their instantaneous tangency to the flow velocity vector. These streamlines were visualized on a vertical plane positioned along the truck, originating from the plane edge. Figures 12 and 13 present a comparison of velocity streamlines for two deflector designs in three distinct positions. Figure 12 depicts the high-velocity streamlines ahead of and behind the baseline model. For the baseline model, the drag force in this configuration was calculated as  $2371.03\text{ N}$ , with a corresponding drag coefficient of  $0.515$ .

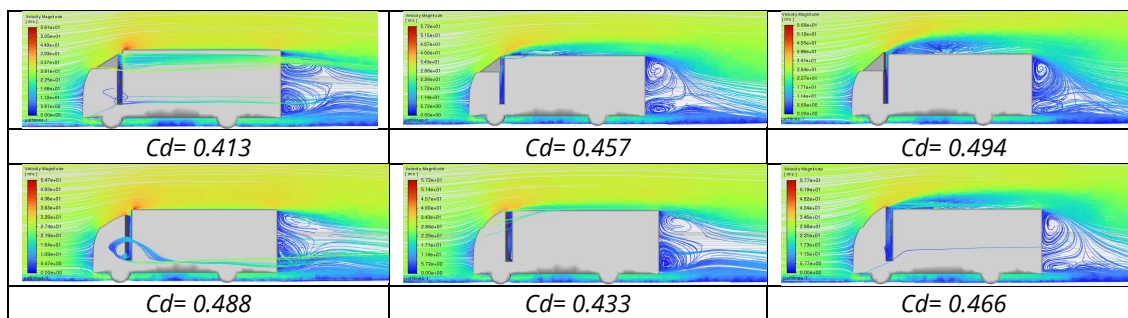


$Cd = 0.515$

**Fig. 12** Streamline visualization on a basic model

Figure 13 demonstrates that, in all cases, the drag coefficient ( $Cd$ ) of the modified model is lower than that of the basic model, suggesting a significant aerodynamic contribution from the air deflector, consistent with findings from prior studies [15, 24, 25]. A drag analysis was conducted on both the basic and modified trailer truck models, with drag coefficients measured in terms of  $Cd$ . The results revealed  $Cd$  values of  $0.515$  for the basic model and  $0.413$  for the modified model, indicating that the profile modifications substantially reduced aerodynamic drag.

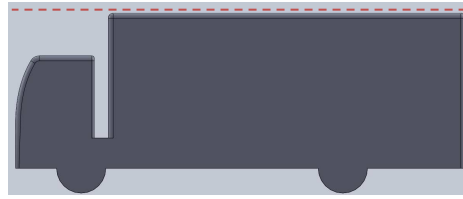
Figure 13 further illustrates a comparison of airflow streamlines across six cases for a truck equipped with two air deflector models (designs) positioned at three distinct locations. Additionally, Figure 14 depicts the influence of rear vanes on turbulence control at the rear of the truck. Notably, turbulent flow is significantly reduced in Cases 2 and 5. Conversely, substantial turbulent flow is observed behind the truck and above the container in Cases 3 and 6. Furthermore, turbulent flow between the cabin and the container is evident in Cases 1 and 4.



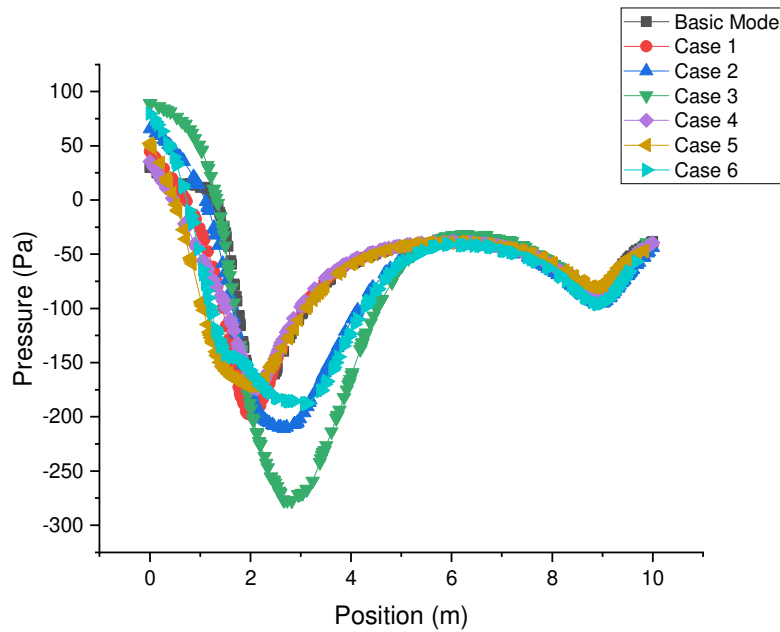
**Fig. 13** Comparison of streamline in different cases

Figure 14 illustrates the variation of pressure, velocity, and turbulence along a position line extending over the length of the truck.

Figure 15 illustrates the pressure variation as a function of position along the truck's length. From this figure, it can be observed that the pressure variation is more non-uniform for all cases, especially for cases 2, 3, and 6, while the base model shows only a small variation. The pressure is found to be reduced at the front of the truck equipped with an air deflector due to its aerodynamic shape. At the rear of the truck, the pressure decreases further, thereby reducing the tendency for wake formation.



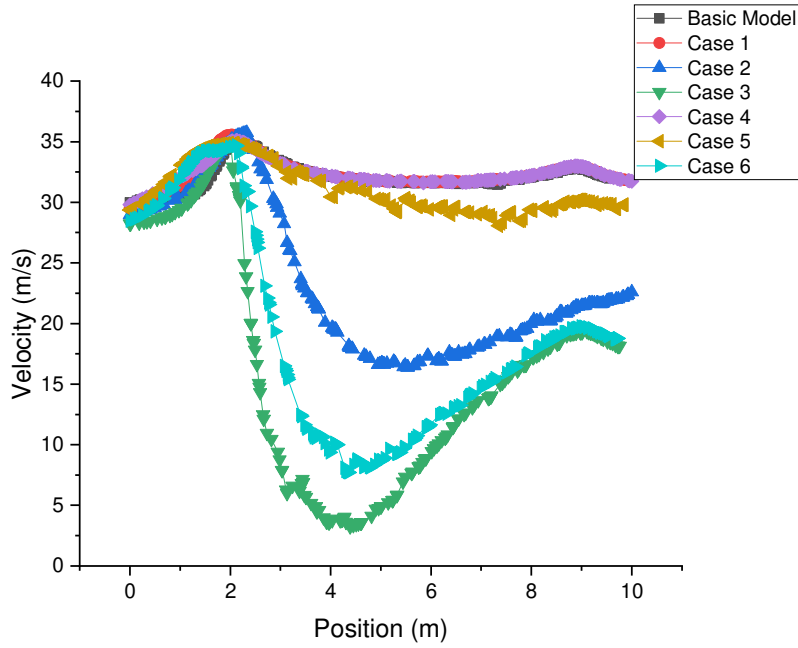
**Fig. 14** Position line extending over the length of the truck



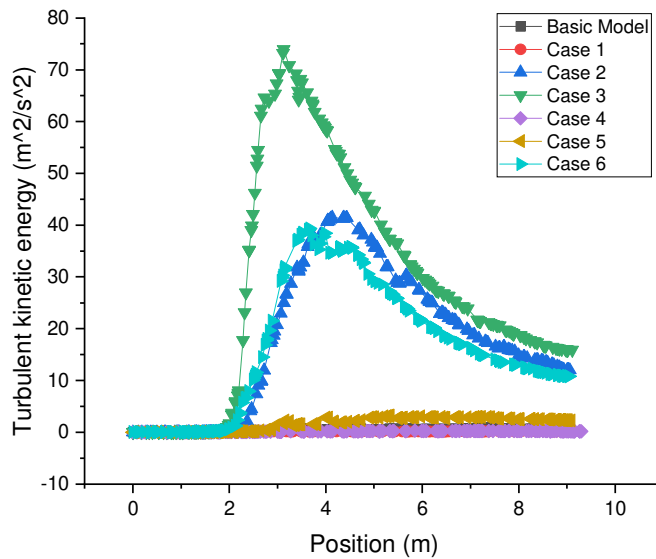
**Fig. 15** Pressure curve as a function of position of different cases

Figure 16 illustrates the variation of velocity as a function of position along the truck's length. From this figure, it can be observed that the variation of velocity is nearly uniform for the base model as well as for cases 1, 4, and 5. However, cases 2, 3, and 6 exhibited variations compared to the base model. The velocity is found to be reduced in cases 2, 3, and 6 immediately after the air deflector, due to its shape and installation above the container. The pressure remains low at the rear of the truck in cases 2, 3, and 6 compared to the base model.

Figure 17 shows the variation of turbulent kinetic energy as a function of position along the truck's length. The behaviour of the curves in this figure is almost the opposite of that observed in the previous figure (Figure 15, velocity). It can be seen that the turbulent kinetic energy remains stable and nearly zero for cases 1, 4, 5, as well as for the base model, along the line positioned above the truck (in the middle, at a height of  $3.617\text{ m}$ ). On the other hand, it reaches a maximum peak at a position of  $3\text{ m}$  immediately after the air deflector for cases 2 and 6, and especially for case 3. This difference results from the shape (model) of the air deflector and its position.



**Fig. 16** Velocity curve as a function of position of different cases



**Fig. 17** Turbulent kinetic energy curve as a function of position of different cases

The drag values generated for each case are shown in Table 2. The drag coefficient reduction is evaluated compared to the base model. It can be observed that that the drag coefficient reduction for the first case (first model in first position) is 19.80% compared to 18.88% at 30 m/s as reported DANG, Tien Phuc et al [26], and followed by the fifth case, 15.92% (second model in second position).

**Table 2** Table of drag force and coefficient

Cases	drag force (N)	drag coefficient	drag coefficient reduction
Basic model	2371.03	0.515	
Case 1	1901.79	0.413	19.80 %
Case 2	2103.88	0.457	11.26 %
Case 3	2329.93	0.494	4.07 %
Case 4	2248.99	0.488	5.24 %
Case 5	1995.54	0.433	15.92 %
Case 6	2212.07	0.466	9.51 %

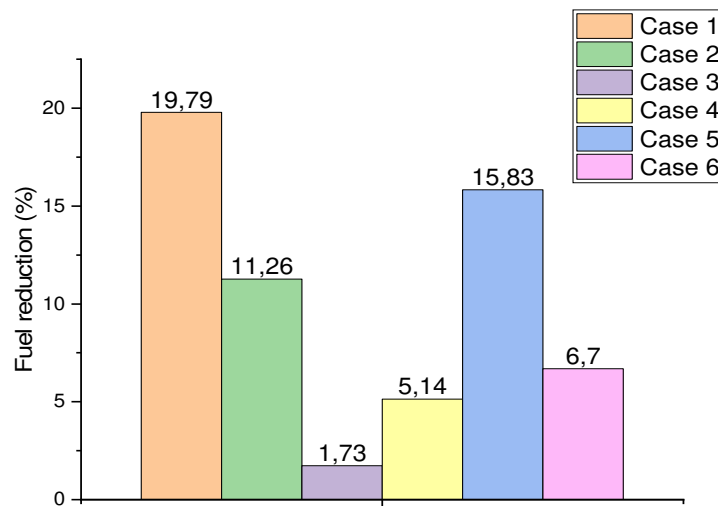


**Fig. 18** Percentage reduction in fuel consumption

Their aerodynamics influences fuel consumption in trucks; the more drag a truck generates, the more fuel it requires to travel. Figure 18 shows a comparison of fuel consumption. It is found that the use of an air deflector can reduce the fuel consumption of trucks by up to 19.79% compared to the base model (truck without a deflector). In addition, it is observed that the shape and position of the deflector directly affect fuel consumption. The drag force and drag coefficient directly influence the percentage of fuel consumption decrease, which varies depending on the circumstances, as mentioned in previous studies [10, 11, 26, 27]. These findings also suggest that the truck's fuel efficiency could be considerably increased by installing a drag reduction device [17].

#### 4. CONCLUSIONS

This paper presents a comparative study between the basic design of a heavy-duty truck (basic model) and a heavy-duty truck equipped with deflectors, analysed through six cases to reduce aerodynamic drag. Two deflector designs are proposed and investigated using CFD simulations. The CFD analysis of the six configurations, as well as the basic model, is carried out using the standard k-ε turbulence model.

The addition of air deflectors on the basic truck model results in a drag reduction ranging from 4.07% to 19.80%, and a drag force reduction ranging from 1.73% to 19.79%. These improvements lead to better fuel efficiency, with reduced fuel consumption.

The simulations indicate that:

- 1 - The air deflector plays a crucial role in improving aerodynamics and reducing drag force.
- 2 - A significant drag reduction was observed in cases 1 and 5.
- 3 - Airflow and pressure distribution analyses indicate that the shape of the deflector is the main factor in aerodynamic improvement, followed by its position.
- 4 - A reduction in fuel consumption was observed, directly related to the improvement in aerodynamics and the reduction in drag force.

In future work, we aim to optimize the shape of the air deflector and validate our results experimentally using a wind tunnel.

## 5. REFERENCES

- [1] Gao, W., Deng, Z., He, Y., A comparative study of tail air-deflector designs on aerodynamic drag reduction of medium-duty trucks, *International Journal of Vehicle Performance*, Vol. 8, No. 2-3, pp. 316-333, 2022. <https://doi.org/10.1504/IJVP.2022.122138>
- [2] Chaichan\*, M.T., Fayad, M.A., Al Ezzi, A., Dhahad, H.A., Megaritis, T., Yusaf, T., Al-Amiery\*, A., Wan Isahak, W.N.R., Ultralow sulfur diesel and rapeseed methyl ester fuel impact on performance, emitted regulated, unregulated, and nanoparticle pollutants, *ACS omega*, Vol. 7, No. 30, pp. 26056-26075, 2022. <https://doi.org/10.1021/acsomega.2c00893>
- [3] Fayad, M.A., Radhi, A.A., Omran, S.H., Mohammed, F.M., Influence of environment-friendly fuel additives and fuel injection pressure on soot nanoparticles characteristics and engine performance, and NOX emissions in CI diesel engine, *Journal of Advanced Research in Fluid Mechanics and Thermal Sciences*, Vol. 88, No. 1, pp. 58-70, 2021. <https://doi.org/10.37934/arfmts.88.1.5870>
- [4] Curry, T., Liberman, I., Hoffman-Andrews, L., Lowell, D., Reducing Aerodynamic Drag & Rolling Resistance from Heavy-Duty Trucks: Summary of Available Technologies & Applicability to Chinese Trucks, International Council on Clean Transportation One Hallidie Plaza Suite 503 San Francisco, CA 94102. [www.theicct.org](http://www.theicct.org)
- [5] Xie, X., Hu, S., Chen, W., Chen, Y., Wang, H., Hao, L., Aerodynamic optimization of tail-board in heavy-duty truck based on approximate model and non-smooth surface, In: Proceedings of China SAE Congress 2020: Selected Papers. Singapore : Springer Nature Singapore, pp. 369-386, 2022. [https://doi.org/10.1007/978-981-16-2090-4\\_21](https://doi.org/10.1007/978-981-16-2090-4_21)
- [6] Schoon, R.E., On-road evaluation of devices to reduce heavy truck aerodynamic drag, SAE Technical Paper, 2007. <https://doi.org/10.4271/2007-01-4294>
- [7] Kim, J.J., Kim, J., Hann, T., Kim, D., Roh, H.S., Lee, S.J., Considerable drag reduction and fuel saving of a tractor-trailer using additive aerodynamic devices, *Journal of Wind Engineering and Industrial Aerodynamics*, Vol. 191, pp. 54-62, 2019. <https://doi.org/10.1016/j.jweia.2019.05.017>

- [8] Hariram, A., Koch, T., Mårdberg, B., Kyncl, J., A study in options to improve aerodynamic profile of heavy-duty vehicles in Europe, *Sustainability*, Vol. 11, No. 19, 5519, 2019. <https://doi.org/10.3390/su11195519>
- [9] Zhang, Q., Su, C., Zhou, Y., Zhang, C., Ding, J., Wang, Y., Numerical investigation on handling stability of a heavy tractor semi-trailer under crosswind, *Applied Sciences*, Vol. 10, No. 11, 3672, 2020. <https://doi.org/10.3390/app10113672>
- [10] Connolly, M.G., O'Rourke, M.J., Ivankovic, A., Drag reduction technology and devices for road vehicles-A comprehensive review, *Heliyon*, 2024. <https://doi.org/10.1016/j.heliyon.2024.e33757>
- [11] Kim, J.J., Lee, S., Kim, M., You, D., Lee, S.J., Salient drag reduction of a heavy vehicle using modified cab-roof fairings, *Journal of Wind Engineering and Industrial Aerodynamics*, Vol. 164, pp. 138-151, 2017. <https://doi.org/10.1016/j.jweia.2017.02.015>
- [12] Dhumal, A., Ambhore, N., Tamkhade, P., Marne, A., Muzawar, N., Numerical Optimization for Aerodynamic Performance of Nose Cone of FSAE Vehicle through CFD, *CFD Letters*, Vol. 16, No. 11, pp. 161-171, 2024. <https://doi.org/10.37934/cfdl.15.11.161171>
- [13] Nishanth, P., Haseebuddin, M.R., Srinath, P., Saleel, N., Hegde, P., Das, A.N.M., Aerodynamic Drag Reduction of 3D Printed Bus Model and Substantiation Using Wind Tunnel, *Journal of The Institution of Engineers (India): Series D*, pp. 1-13, 2023. <https://doi.org/10.1007/s40033-023-00540-4>
- [14] Halfina, B., Hendrato, Depari, Y.P.D.S., Muhammad, Kurnia, S.H.M., Fitri, H.A., Numerical Analysis for Different Masks of Car Design of High-Speed Train, *International Journal of Automotive and Mechanical Engineering*, Vol. 19, No. 4, pp. 10144-10151, 2022. <https://doi.org/10.15282/ijame.19.4.2022.11.0785>
- [15] Farghaly, M.B., Sarhan, H.H., Abdelghany, E.S., Aerodynamic performance enhancement of a heavy trucks using experimental and computational investigation, *CFD Letters*, Vol. 15, No. 8, pp. 73-94, 2023. <https://doi.org/10.37934/cfdl.15.8.7394>
- [16] <https://grabcad.com/library/ford-cargo-1113-1>
- [17] Roy, S., and Srinivasan, P., External flow analysis of a truck for drag reduction, *SAE transactions*, pp. 808-812, 2000. <https://doi.org/10.4271/2000-01-3500>
- [18] Hjelm, L., Bergqvist, B., European truck aerodynamics—a comparison between conventional and coe truck aerodynamics and a look into future trends and possibilities, In: *The Aerodynamics of Heavy Vehicles II: Trucks, Buses, and Trains*, Berlin, Heidelberg: Springer Berlin Heidelberg, pp. 469-477, 2009. [https://doi.org/10.1007/978-3-540-85070-0\\_45](https://doi.org/10.1007/978-3-540-85070-0_45)
- [19] Wong, J., *Theory of Ground Vehicles*, Fourth Edition, John Wiley & sons, Inc., 2008.
- [20] Hammad, M., He, Y., A review of active aerodynamic control for increasing safety of high-speed road vehicles, In: *Proceedings of The Joint Canadian Society for Mechanical Engineering and CFD Society of Canada International Congress 2019*.
- [21] Ghurri, A., Alim, M., Adi, M.N.P., Putra, S.G.B., Mantik, M.E., Suharto, S., Anderson, R., CFD Simulation of Aerodynamics Truck Using Cylinder as Drag Reduction Device, *Journal of Advanced Research in Fluid Mechanics and Thermal Sciences*, Vol. 105, No. 2, pp. 166-181, 2023. <https://doi.org/10.37934/arfmts.105.2.166181>

- [22] Humphreys, H., Batterson, J., Bevly, D., Schubert, R., An evaluation of the fuel economy benefits of a driver assistive truck platooning prototype using simulation, *SAE Technical Paper*, 2016. <https://doi.org/10.4271/2016-01-0167>
- [23] Jiang, M., Wu, H., Tang, K., Kim, M., et al., Evaluation and Optimization of Aerodynamic and Aero- Acoustic Performance of a Heavy Truck using Digital Simulation, *SAE International Journal of Passenger Cars-Mechanical Systems*, Vol. 4, No. 2011-01-0162, 143-155, 2011. <https://doi.org/10.4271/2011-01-0162>
- [24] Khosravi, M., Mosaddeghi, F., Oveisi, M., Ali khodayari-b, Aerodynamic drag reduction of heavy vehicles using append devices by CFD analysis, *Journal of Central South University*, Vol. 22, pp. 4645-4652, 2015. <https://doi.org/10.1007/s11771-015-3015-7>
- [25] Chilbule, C., Upadhyay, A., Mukkamala, Y., Analyzing the profile modification of truck-trailer to prune the aerodynamic drag and its repercussion on fuel consumption, *Procedia Engineering*, Vol. 97, pp. 1208-1219, 2014. <https://doi.org/10.1016/j.proeng.2014.12.399>
- [26] Dang, T.P., Nguyen, X.N., Tran, V.H., Comparison of Aerodynam Characteristics With and Without Wind Deflector for Truck, In: *The International Conference on Sustainable Energy Technologies*. Singapore: Springer Nature Singapore, pp. 485-493, 2023. [https://doi.org/10.1007/978-981-97-1868-9\\_49](https://doi.org/10.1007/978-981-97-1868-9_49)
- [27] Mohamed-Kassim, Z., Filippone, A., Fuel savings on a heavy vehicle via aerodynamic drag reduction, *Transportation Research Part D: Transport and Environment*, Vol. 15, No. 5, pp. 275-284, 2010. <https://doi.org/10.1016/j.trd.2010.02.010>